THE JOURNAL OF PHYSICAL CHEMISTRY C

Article

Cite This: J. Phys. Chem. C 2019, 123, 21022−21030

pubs.acs.org/JPCC

Syngas Conversion to C_2 Oxygenates over the Cu/β-Mo_2C Catalyst: Probing into the Effect of the Interface between Cu and β-Mo_2C on Catalytic Performance

Riguang Zhang,[†] Cong Wei,[†] Weisheng Guo,[†] Zhiqin Li,[‡] Baojun Wang,*[,†] Lixia Ling,[†] and Debao Li[§]

[†]Key Laboratory of Coal Science and Technology of Ministry of Education and Shanxi Province, Taiyuan University of Technology, Taiyuan 030024, Shanxi, P. R. China

[‡]College of Chemistry and Chemical Engineering, Xi'an Shiyou University, Xi'an 710065, Shaanxi, P. R. China

[§]State Key Laboratory of Coal Conversion, Institute of Coal Chemistry, Chinese Academy of Sciences, Taiyuan 030001, Shanxi, P. R. China

Supporting Information

ABSTRACT: Aiming at probing into the role of the interface between Cu and Mo_2C for syngas conversion to C_2 oxygenates over the Cu/β-Mo_2C catalyst, the formation mechanism of C_2 oxygenates from syngas over the Cu/β-Mo_2C catalyst has been systematically investigated using density functional theory calculations. The results show that the CH monomer is the most preferred CH_x species formed via the route of CO direct dissociation into C, followed by C hydrogenation to CH; moreover, the Cu/β-Mo_2C(001) catalyst presents higher activity and selectivity toward CH formation instead of CH_3OH formation. For C_2 oxygenate formation, CHO insertion into CH to form the C_2 oxygenate CHCHO is the most preferred. Compared to the pure Cu(111) and β-Mo_2C(001), Cu/β-Mo_2C(001) exhibits better selectivity toward CH formation, and has the strong ability of C−C chain growth for C_2 oxygenate formation. On the other hand, the analysis of electronic and structural properties indicates that there is a strong charge transfer between Cu and Mo_2C to form a charge-rich region at the interface of the Cu/β-Mo_2C(001) catalyst, which promotes the C−O bond cleavage of CO and CHO to form the CH monomer adsorbed at the interface, and favors the subsequent CHO insertion into CH to form the C_2 oxygenate CHCHO at the interface. As a result, the synergistic effect including the electronic and geometric effect that occurred at the interface between Cu and β-Mo_2C(001) leads to high productivity toward C_2 oxygenates in syngas conversion over the Cu/β-Mo_2C(001) catalyst.

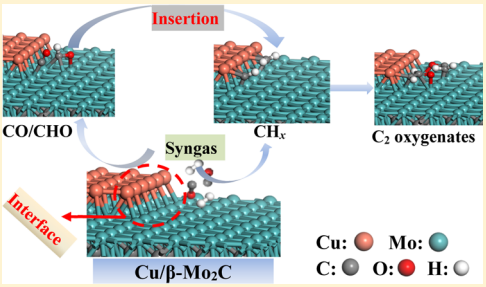

1. INTRODUCTION

Syngas (CO + H_2) conversion into C_2 oxygenates (ethanol, acetaldehyde, and acetic acid) is a potential route to develop novel energy.[1−4] To develop a catalyst with high activity and selectivity, syngas conversion to C_2 oxygenates is necessary.[4] Nowadays, there are four types of typical catalysts, Cu-based catalysts,[5] Rh-based catalysts,[6,7] Mo-based catalysts,[8] and modified Fischer−Tropsch synthesis catalysts.[9−11] Among them, Rh-based catalysts were considered to be the most promising; however, the high cost and low CO conversion rate limit its application in industry. Recently, the Cu catalyst has been widely used in syngas conversion because of low cost, high CO conversion rate, and the easier formation of C_2 oxygenates once CH_x species was formed;[3] however, it is difficult for the formation of CH_x species because of the unfavorable C−O bond cleavage, and leads to high selectivity of methanol and low selectivity of C_2 oxygenates, which was attributed to the low concentration of CH_x for C−C chain growth.[12] Density functional theory (DFT) studies indicated that CH_3OH formation was more favorable than CH_x species formation on the Cu(111),[13] Cu(110),[14] and Cu(100)[15] surfaces. Experiments combined with DFT calculations by Sun et al.[16] proved that the promoter Cs-modified Cu catalyst exhibited high activity toward ethanol formation. Thus, it is necessary to introduce the promoter to modify the Cu catalyst; up to now, Co−Cu,[9−11] Cu−Cs,[16] and Rh−Cu[17] bimetallic catalysts have exhibited better selectivity toward C_2 oxygenates.

For the Mo-based catalyst, Mo_2C was often used as an active component and support for syngas conversion, which dominantly resulted in the formation of hydrocarbons.[18,19] Shou et al.[20] experimentally found that Mo_2C was more active for hydrocarbon formation with the selectivity of 89.0%. Li and Sholl[21] theoretically investigated syngas conversion on the hexagonal Mo_2C(001) surface, indicating that the selectivity of total hydrocarbons was 82.9%. Ranhotra et al.[22] experimentally showed that the hexagonal Mo_2C exhibited high selectivity

Received: June 23, 2019
Revised: July 29, 2019
Published: August 1, 2019

DOI: 10.1021/acs.jpcc.9b05963
J. Phys. Chem. C 2019, 123, 21022−21030

toward olefin. Christensen et al.[23] revealed that K_2CO_3/Mo_2C had better performance than K_2CO_3/WC and NbC catalysts for mixed alcohol; further, Cu-modified K_2CO_3/Mo_2C improved the selectivity toward ethanol. The above results show that Mo_2C was in favor of the formation of the hydrocarbons and higher alcohols, which means that Mo_2C first favors syngas conversion to form CH_x species, which was the necessary species for the formation of hydrocarbons and higher alcohols in syngas conversion.

Recently, supported Cu catalysts have been widely used including SiO_2,[24] CeO_2,[25] Al_2O_3,[26] TiO_2,[27,28] AlOOH,[29,30] and ZnO supporters.[31] For example, Rodriguez et al.[28] theoretically investigated the activity of Cu and Au nanoparticles deposited over the $TiO_2(110)$ surface for water gas shift reaction (WGS), suggesting that $Cu/TiO_2(110)$ exhibited better catalytic activity than $Au/TiO_2(110)$. DFT studies by Bai et al.[29,30] verified that Cu/AlOOH(001) was more favorable for ethanol formation than AlOOH(001). Yang et al.[31] experimentally and theoretically revealed that the catalytic activity of Cu/ZnO(000−1) was higher than Cu(111) for methanol formation via CO_2 hydrogenation. On the other hand, a bifunctional catalyst could be formed by loading metals onto the supports, in which the interface between the metal and the support played a key role in many reactions because of the new adsorption sites and unique electronic properties.[32−34] Our previous DFT study[35] showed that a Cu strip deposited on an χ-$Fe_5C_2(510)$ surface exhibited better selectivity toward higher alcohol in syngas conversion because of the synergistic interaction at the interface between Cu and Fe_5C_2. Zhou et al.[36] experimentally found that CeO_2-supported Rh particles could promote methanol decomposition that occurred at the Rh−CeO_2 interface. Chen et al.[37] experimentally revealed that the interface Co/CoO_x was devoted to higher alcohol formation; the synergistic effect of Co and CoO_x was that Co promoted CH_x formation and CoO_x provided undissociative CO, which led to high alcohol selectivity. Similar results by Pei et al.[38] revealed that the interface between Co and Co_2C could promote the formation of higher alcohols, the undissociative CO was adsorbed at the Co_2C, and Co promoted the C−O bond cleavage of CO to form CH_x species. Up to now, the transition metal supported on Mo_2C was used in syngas conversion to form alcohol and hydrocarbons. Xiang et al.[39] experimentally investigated the formation of higher alcohol over the Fe, Ni, and Co-modified K/β-Mo_2C catalyst; KNi/Mo_2C and KCo/Mo_2C catalysts showed better behavior toward higher alcohol. Dong et al.[40] experimentally showed that the strong interaction between Au and Mo_2C produced high dispersion of Au; the Au/MoC_x catalyst exhibited high activity for WGS reactions. Schweitzer et al.[41] experimentally and theoretically revealed that the Pt/Mo_2C catalyst exhibited higher activity toward WGS reaction than Pt/CeO_2 and Pt/TiO_2 as the interface between Mo_2C and Pt could provide more active sites. Posada-Pérez et al.[42] showed that the interface of Cu/Mo_2C provided a new route for CO_2 hydrogenation to CH_3OH, and the role of Cu was to inhibit CH_4 formation.

As the mechanism of C_2 oxygenate formation is known to include two steps, one being CO activation to form CH_x species and the other being CO/CHO insertion into CH_x,[43,44] the co-existence of CH_x species from CO dissociation and the undissociated CO/CHO species is necessary. Thus, the dual active sites must be required for C_2 oxygenate formation in syngas conversion. On the basis of the above analysis, taking the advantages of Cu and Mo_2C in syngas conversion into consideration, it is therefore assumed that the Cu/Mo_2C catalyst should be considered as a potential material, in which the synergistic interaction at the interface between Cu and Mo_2C may be in favor of syngas conversion to form C_2 oxygenates. However, until now, few research studies have focused on the Cu/Mo_2C catalyst for C_2 oxygenate formation from syngas. As a result, two key issues cannot be answered: can the interface between Cu and the Mo_2C in the Cu/Mo_2C catalyst enhance the catalytic performance for C_2 oxygenate formation? What is the role of Cu and Mo_2C in syngas conversion to C_2 oxygenates?

In this study, aiming at illustrating the above two issues, the formation mechanism of C_2 oxygenates from syngas has been systematically investigated over Cu/Mo_2C catalysts, including CO initial activation, CH_x formation, and CO/CHO insertion into CH_x to form the C_2 oxygenates CH_xCO/CH_xCHO. Moreover, the comparisons among Cu, Mo_2C, and Cu/Mo_2C catalysts are carried out to identify the roles of Cu and Mo_2C, as well as the synergetic interaction at the interface of Cu and Mo_2C. It is hoped that this study could give out a valuable clue for the design and optimization of Cu/Mo_2C catalysts in syngas conversion to form C_2 oxygenates.

2. MODEL AND COMPUTATIONAL DETAILS

2.1. Calculation Model. For the Mo_2C catalyst, the hexagonal phase (α-Mo_2C) and the orthorhombic phase (β-Mo_2C) exist; α-Mo_2C is unstable at high temperatures.[44−46] However, Politi et al.[47] theoretically investigated the geometric and electronic structure of bulk and low Miller-index β-Mo_2C surfaces; it was found that β-Mo_2C had a stronger metallic character than α-Mo_2C; meanwhile, the (011) surface was nonpolar and the most stable of β-Mo_2C, whereas the polar (001) surface has cleavage energies comparable to those of the (111) surface; namely, the sub-stable (001) surface has better catalytic activity than the stable (011) surface. Moreover, the adsorption of small molecules (O_2, CO, CO_2, H, CH_x (x = 0−3), C_2H_4) on β-$Mo_2C(001)$ [α-$Mo_2C(0001)$ in their notation] have been also performed using DFT calculations.[48,49] The studies by Tominaga and Nagai focused on the individual reaction steps associated with several reactions on β-Mo_2C-(001) including the WGS reaction,[50] CH_4 reforming,[51] and hydrodesulfurization of thiophene.[52] Among these studies, the (001) surface is given special attention as it is the most densely packed surface of β-Mo_2C. Further, Posada-Pérez et al.[53] experimentally and theoretically found that the Mo-terminated β-$Mo_2C(001)$ polar surface easily adsorbed and decomposed CO_2 into CO than the C-terminated β-$Mo_2C(001)$ polar surface. At the same time, the work by Posada-Pérez et al.[34] reported CO_2 hydrogenation to methanol over the β-$Mo_2C(001)$ surface, suggesting that the Mo-terminated β-$Mo_2C(001)$ surface easily dissociated CO_2 at low temperatures and the CO produced also decomposed into C and O adatoms by overcoming a relatively small energy barrier compared to the C-terminated β-$Mo_2C(001)$ surface, suggesting that the Mo-terminated β-$Mo_2C(001)$ surface was an ideal active surface. In addition, under the hydrogen-rich conditions of syngas conversion, the surface C of C-terminated β-Mo_2C-(001) may be easily hydrogenated to form CH_x (x = 1−3), which weakens the strength of the Mo−C bond and leads to the unstable existence of the C-terminated β-$Mo_2C(001)$ surface. Thus, the Mo-terminated β-$Mo_2C(001)$ surface is

DOI: 10.1021/acs.jpcc.9b05963
J. Phys. Chem. C 2019, 123, 21022−21030

selected to represent the Mo_2C catalyst in syngas conversion under hydrogen-rich conditions.

The structure of the four-atom Cu (Cu_4) cluster including the tetrahedral and planar were used to model the Cu component supported over the Mo-terminated β-$Mo_2C(001)$ surface. Our calculated results show that the tetrahedral Cu_4 cluster supported over the Mo-terminated β-$Mo_2C(001)$ surface will turn into the planar Cu_4 cluster after optimization, which is in agreement with previous studies.[42] Thus, the planar Cu_4 cluster is the most stable configuration over the Mo-terminated β-$Mo_2C(001)$ surface, as shown in Figure 1; the Cu_4 cluster supported over the Mo-terminated β-$Mo_2C(001)$ is chosen to model the Cu/Mo_2C catalyst in this study, which is named as Cu/β-$Mo_2C(001)$.

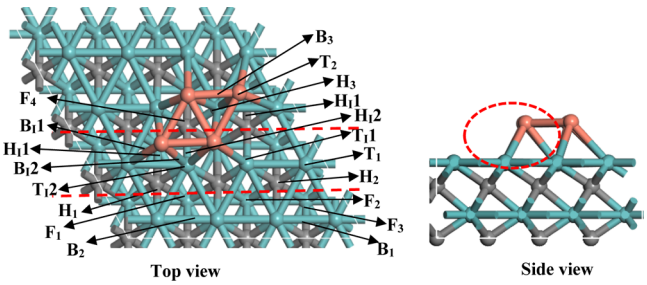

Figure 1. Top and side views of the Cu/β-$Mo_2C(001)$ surface; the orange, gray, and cyan spheres represent Cu, C, and Mo atoms, respectively. H, F, B, and T represent the hcp, fcc, bridge, and top sites, respectively; T_I, B_I, and F_I represent the top, bridge, and threefold site of the interface, respectively; the red area is the interface consisting of Cu and β-$Mo_2C(001)$.

2.2. Calculation Method. All calculations were performed using the DFT method, which was implemented by the Vienna Ab initio Simulation Package.[54,55] The electron exchange correlation energy was treated within the generalized gradient approximation with the Perdew−Burke−Ernzerhof functional.[56] The *k*-point meshes were 3 × 3 × 1, and the thickness of vacuum was 15 Å to prevent interaction between the slabs; the plane wave cutoff energy was 400 eV.[57,58] The convergence criterion on the force of geometry optimization and the transition state (optimized by dimer method) were lower than 0.05 eV·$Å^{-1}$.[59,60] The saddle point between the initial state and final state was found out by the climbing-image nudged elastic band method.[61,62] In addition, the vibrational frequency was also calculated to confirm the transition state with the only one imaginary frequency.

The syngas conversion on Mo_2C usually occurred at 573 K[20,21] and that on the Cu-based catalyst was in the temperature range of 553−583 K.[3] Considering the temperature of syngas conversion over the Co and Mo_2C catalysts, 573 K was selected in this study as the reaction temperature for syngas conversion to C_2 oxygenates over the Cu/β-$Mo_2C(001)$ catalyst. Thus, all thermodynamic quantities involving the elementary reactions of syngas conversion to C_2 oxygenate were computed at 573 K (see details in the Supporting Information).

3. RESULTS AND DISCUSSION

Generally, syngas conversion to C_2 oxygenates includes three key steps: CO initial activation, CH_x (x = 1−3) formation, and CHO/CO insertion into CH_x. Meanwhile, methanol (CO hydrogenation) and hydrocarbons (CH_x hydrogenation or self-coupling) are produced to decrease the selectivity of C_2 oxygenates. Thus, these above reactions are considered on the Cu/Mo_2C catalyst, which will contribute to the understanding about the catalytic performance of the Cu/β-$Mo_2C(001)$ catalyst in syngas conversion to C_2 oxygenates.

Table 1. Related Reactions Involved in Syngas Conversion to C_2 Oxygenates Together with the Corresponding Activation Free Energy (ΔG_a/kJ·mol^{-1}) and Reaction Free Energy (ΔG/kJ·mol^{-1}) at 573 K on the Cu/β-$Mo_2C(001)$ Surface[a]

	elementary reaction	ΔG_a	ΔG	ν
R1	CO → C + O	116.4(113.5)	−120.3(−122.4)	330.8i
R2	CO + H → CHO	116.8(97.8)	96.9(78.0)	54.0i
R3	CO + H → COH	218.5(196.3)	99.8(91.6)	1378.1i
R4	C + H → CH	101.5(101.0)	15.3(11.8)	900.9i
R5	CHO + H → CH_2O	76.4(106.5)	18.2(26.3)	889.0i
R6	CHO + H(1) → CHOH	154.2(156.9)	66.8(55.0)	1370.3i
R7	CH_2O + H → CH_3O	115.9(95.4)	22.1(−4.2)	962.2i
R8	CH_2O + H(1) → CH_2OH	148.6(144.4)	66.9(49.2)	1318.1i
R9	CHO → CH + O	34.3(54.5)	−197.5(−192.0)	267.1i
R10	CH_3O + H → CH_3OH	239.5(235.3)	139.1(121.4)	1318.1i
R11	CH + H → CH_2	120.8(118.0)	58.3(50.5)	829.0i
R12	CH + CH → C_2H_2	131.9(128.7)	18.4(10.4)	150.0i
R13	CH + CO → CHCO	143.8(134.5)	71.6(63.2)	295.3i
R14	CH + CHO → CHCHO	51.2(49.1)	−6.9(−7.5)	331.1i
R15	CH_2 + H → CH_3	124.8(120.1)	60.2(49.3)	394.3i
R16	CH_3 + H → CH_4	166.9(168.7)	83.3(95.4)	894.5i
R17	CH_2 + CH_2 → C_2H_4	154.4(154.0)	82.9(62.5)	586.4i
R18	CH_2 + CO → CH_2CO	27.8(14.7)	7.1(−15.4)	335.9i
R19	CH_2 + CHO → CH_2CHO	137.8(113.2)	76.1(58.0)	104.8i
R20	CH_3 + CO → CH_3CO	191.7(180.7)	89.6(74.8)	365.5i
R21	CH_3 + CHO → CH_3CHO	166.3(157.2)	81.2(65.1)	475.9i
R22	CH_3 + CH_3 → C_2H_6	343.7(364.5)	126.6(121.8)	791.9i

[a]It is noted that the values in the parentheses are at 0 K, whereas the values outside the parentheses are at 573 K.

DOI: 10.1021/acs.jpcc.9b05963
J. Phys. Chem. C 2019, 123, 21022−21030

The activation and reaction free energies of all possible elementary reactions on Cu/β-Mo_2C(001) at 573 K are listed in Table 1. In addition, for CHO insertion into CH_x, a large number of previous studies have investigated the formation of C_2 oxygenates over the Rh, Co, CoCu, CuFe, and PdFe catalysts;[43,63−66] the CHO intermediate is similar to the function of the reactants CH_x and CO species; the formation of the CHO intermediate acted as the reactant, which had not been considered.

On the other hand, in our study, only one H atom is present on the surface for each hydrogenation step in C_2 oxygenate formation from syngas, which ignores the effect of the presence of other H atoms on the reactions. Up to now, a large number of studies have investigated CO hydrogenation reactions over Rh-based,[6,7,17,43] Cu-based,[13−15,29,30] Co-based,[33,43] and Mo-based[21,34] catalysts; these studies did not consider the effect of the presence of the H atom on the reaction mechanism, and the results well-clarified the reaction mechanism. Moreover, in each hydrogenation reaction, although there are a lot of energetically stable H species on the surface, when hydrogenation reaction occurs under a realistic condition, only one H adatom interacts with the corresponding adjacent adsorbed species. The above analysis shows that the effect of the presence of H atoms on the reaction mechanism is not obvious under a realistic condition; meanwhile, this study only qualitatively investigates the mechanism of C_2 oxygenate formation from syngas, and the obtained results are reliable using an H atom on the catalyst surface.

3.1. CO Initial Activation. CO initial activation includes CO direct dissociation and CO hydrogenation to CHO or COH. As presented in Figure 2, CO direct dissociation and CO hydrogenation to CHO are two parallel pathways with the corresponding activation free energies of 116.4 and 116.8 kJ·mol^{-1}, respectively, which are much lower than CO hydrogenation to COH (218.5 kJ·mol^{-1}). On the other hand, CO prefers to be adsorbed at the interface Mo site of Cu/Mo_2C, and the C atom of CO direct dissociation is also adsorbed at the interface threefold Mo site. In addition, CO hydrogenation to CHO on the pure β-Mo_2C(001) (Figure S2) is more kinetically favorable than CO direct dissociation and CO hydrogenation to COH (139.6 vs 249.9, 192.7 kJ·mol^{-1}). On the Cu(111),[13] Cu(110),[14] and Cu(100)[15] surfaces, CHO is also the main intermediate of CO initial activation with the activation barrier of 105.8, 100.1, and 100.9 kJ·mol^{-1}, respectively.

Compared to the pure β-Mo_2C(001) and Cu catalysts, the Cu/β-Mo_2C(001) catalyst is more favorable for CO initial activation, especially for CO direct dissociation, namely, the synergetic interaction that occurred at the Cu/Mo_2C interface improved the catalytic activity of CO initial activation.

3.2. CH_x Formation. As mentioned above, CO initial activation on Cu/Mo_2C mainly includes CO + H → CHO and CO → C + O. Thus, CHO and C are selected as the initial species to investigate the formation of CH_x species, which corresponds to two routes; one is the dissociation of CH_xO (x = 1−3) or CH_xOH (x = 1, 2) formed by CHO hydrogenation, the other is the successive hydrogenation of dissociated C.

3.2.1. CH Formation. Starting from the CHO or C species, as shown in Figure 2, our results show that CHO prefers to be dissociated into CH instead of its hydrogenation to form CHOH and CH_2O; the activation free energies of CHO dissociation and C hydrogenation to CH on the Cu/β-Mo_2C(001) catalyst are 34.3 and 101.5 kJ·mol^{-1}, respectively.

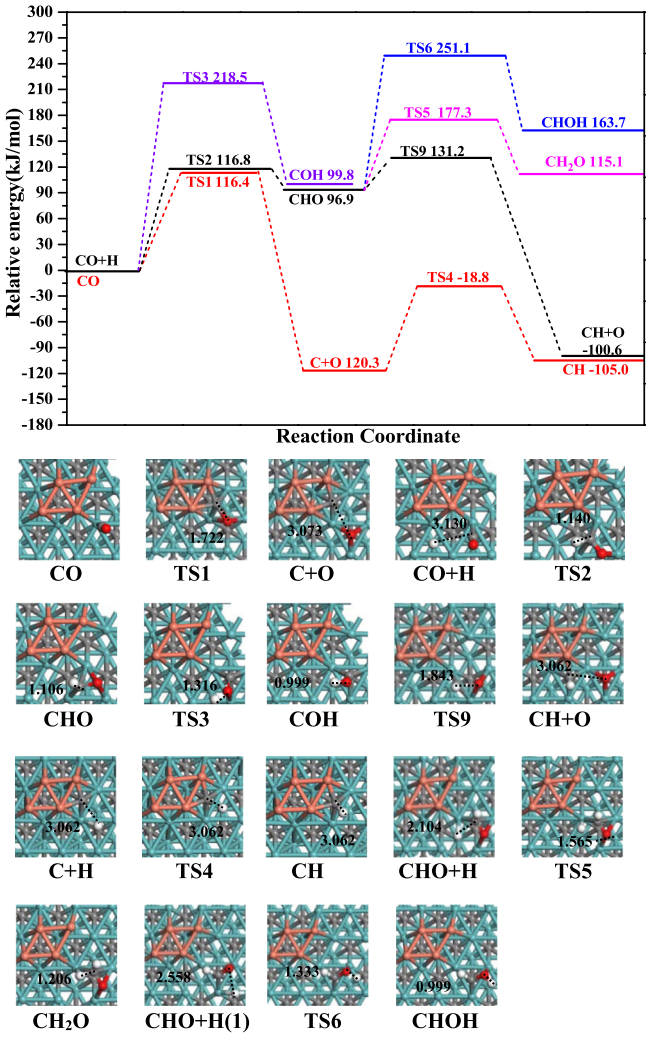

Figure 2. Potential energy diagram of CO initial activation and CH formation together with the structure of the initial state, transition state, and final state on the Cu/β-Mo_2C(001) surface. Bond lengths are in Å. The orange, gray, white, red, and cyan spheres stand for Cu, C, H, O, and Mo atoms, respectively.

The overall barriers of CH formation in these two pathways are 131.2 and 116.4 kJ·mol^{-1}, respectively; namely, the preferred pathway of CH formation is CO direct dissociation into C, followed by C hydrogenation to CH. On the other hand, the activation free energy of CHO dissociation into CH on the pure Mo_2C catalyst is 110.9 kJ·mol^{-1} (see Figure S2), which is much higher than that on the Cu/Mo_2C catalyst (34.3 kJ·mol^{-1}); meanwhile, on the pure Cu catalyst, CHO prefers to be hydrogenated to CH_2O rather than its dissociation into CH.[13] It is noted that compared to the pure Cu and Mo_2C catalysts, CHO prefers to be adsorbed at the sites near the interface region of Cu/Mo_2C, which enhances CHO adsorption ability and promotes CHO dissociation into CH, whereas CHO hydrogenation to form CH_2O or CHOH occurred at the Mo_2C surface.

Thus, the synergetic interaction between Cu and Mo_2C promotes CHO dissociation and improves the catalytic activity and selectivity of CH formation.

3.2.2. CH_2 and CH_3 Formation. Two pathways of CH_2 formation exist; one is the dissociation of CH_2O or CH_2OH from CHO or CHOH/CH_2O hydrogenation, respectively; the

DOI: 10.1021/acs.jpcc.9b05963
J. Phys. Chem. C 2019, 123, 21022−21030

other is CH hydrogenation. As shown in Figure 2, as CHO direct dissociation is more preferred than its hydrogenation to CH_2O and CHOH (34.3 vs 76.4 and 154.2 kJ·mol^{-1}), it is difficult for CH_2 formation via the dissociation of CH_2O or CH_2OH to occur, which should come from CH hydrogenation. Similarly, as CH_3O formation via the pathway of CHO + 2H → CH_2O + H → CH_3O (see Figure 3) cannot

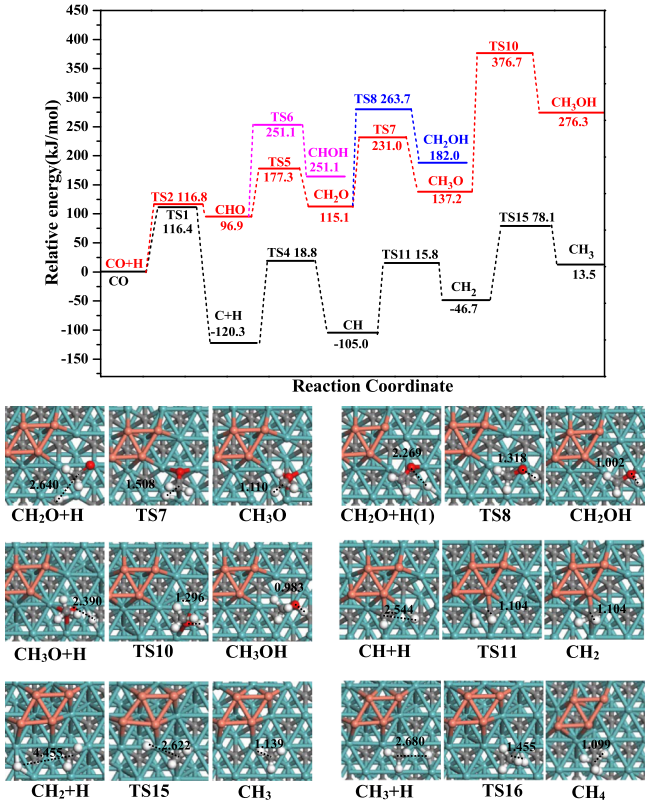

Figure 3. Potential energy diagram for the formation of CH_3OH and CH_4 together with the structure of the initial state, transition state, and final state on the Cu/β-Mo_2C(001) surface. Bond lengths are in Å. See Figure 2 for color coding.

easily occur compared to CHO direct dissociation, CH_3 formation via CH_3O dissociation is also difficult, which also comes from CH_2 hydrogenation. Further, CH hydrogenation to CH_2 and CH_3 is also calculated, as shown in Figure 3; CH_2 and CH_3 formations are strongly endothermic with the corresponding activation free energies of 120.8 and 124.8 kJ·mol^{-1}, respectively; namely, compared to CH formation, CH_2 and CH_3 formation over the Cu/Mo_2C catalyst is unfavorable both kinetically and thermodynamically.

On the basis of the above analysis, it is concluded that the CH monomer is the most preferred CH_x species on the Cu/Mo_2C catalyst, which is dominantly formed by CO direct dissociation into C, followed by its hydrogenation to CH.

3.3. CH_3OH Formation and Its Effect on CH_x Formation. For methanol formation, as shown in Figure 3, CH_3O or CH_2OH hydrogenation is the main route of CH_3OH formation. CHO hydrogenation to CH_2O is more favorable than CHOH formation, starting with the CH_2O species; CH_3O formation is easier than CH_2OH in kinetics with the activation free energies of 115.9 and 148.6 kJ·mol^{-1}, respectively. Therefore, the preferred route of CH_3OH formation is CO + 4H → CHO + 3H → CH_2O + 2H → CH_3O + H → CH_3OH with the overall barrier of 376.7 kJ·mol^{-1}. It is noted that the reactions including CHO hydrogenation to CH_3OH via CH_2O and CH_3O intermediates prefer to occur at the Mo_2C surface. Thus, CH_3OH formation is very unfavorable in kinetics than CH formation (116.4 vs 376.7 kJ·mol^{-1}) on the Cu/Mo_2C catalyst; Cu/β-Mo_2C(001) dramatically promotes CH formation and inhibits CH_3OH production; namely, Cu/β-Mo_2C(001) exhibits high CH selectivity and provides more CH species to take part in the formation of C_2 oxygenates.

Posada-Pérez et al.[34] theoretically investigated CO hydrogenation to methanol on the clean β-Mo_2C(001) surface; the favorable route of methanol formation was similar to that over the Cu/Mo_2C catalyst in this study. On the β-Mo_2C(001) surface, CH_3O is a vital intermediate, which contributes to CH_3OH and CH_3 formation with the activation barriers of 123.5 and 117.7 kJ·mol^{-1}, respectively; namely, CH_3 formation is slightly more favorable than methanol formation in kinetics. On the other hand, previous studies on the Cu(111) surface[13] showed that CH_2 and CH_3 were the preferred CH_x species with the overall barriers of 149.3 and 145.6 kJ·mol^{-1}; however, methanol formation with the overall barrier of 132.0 kJ·mol^{-1} is slightly more favorable than CH_x formation.

The overall formation barriers of the preferred CH_x monomers and CH_3OH over the Cu(111), β-Mo_2C(001), and Cu/β-Mo_2C(001) surfaces are presented in Figure 4.

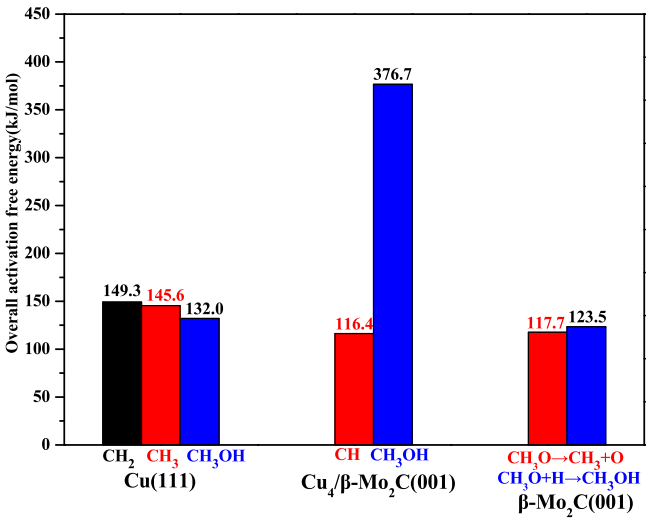

Figure 4. Overall activation free energy for the formation of favored CH_x and CH_3OH over Cu(111),[13] Cu/β-Mo_2C(001), and β-Mo_2C(001) surfaces.[34]

Using the barrier difference between the favored CH_x monomer and methanol as the descriptor is a better method to evaluate the selectivity of the favored CH_x monomer. The more negative barrier difference indicates that CH_x is easily formed, and methanol selectivity is lower. The difference of the overall barriers over the Cu(111), Cu/β-Mo_2C(001), and β-Mo_2C(001) surfaces are 17.3, −260.3, and −5.8 kJ·mol^{-1}; namely, in the Cu/β-Mo_2C catalyst, the synergistic effect of Cu and Mo_2C exhibits higher selectivity toward CH formation instead of CH_3OH, which has little effect on CH formation.

3.4. C_2 Oxygenate Formation. Previous studies[43,44] have verified that the C−C chain formation of C_2 oxygenates mainly goes through CHO/CO insertion into CH_x, which was a vital step to improve the selectivity of C_2 oxygenates. However,

DOI: 10.1021/acs.jpcc.9b05963
J. Phys. Chem. C 2019, 123, 21022−21030

once CH_x is generated, the related reactions of CH_x will occur including CH_x hydrogenation to CH_4, CH_x self-coupling to hydrocarbons, and CHO/CO insertion into CH_x to C_2 oxygenates. As the CH monomer is the dominant CH_x species over Cu/β-Mo_2C(001), starting with the CH species, the related reactions of CH are considered.

As shown in Figure 5, the adsorption configurations of reactants, intermediates, and products indicate that the related

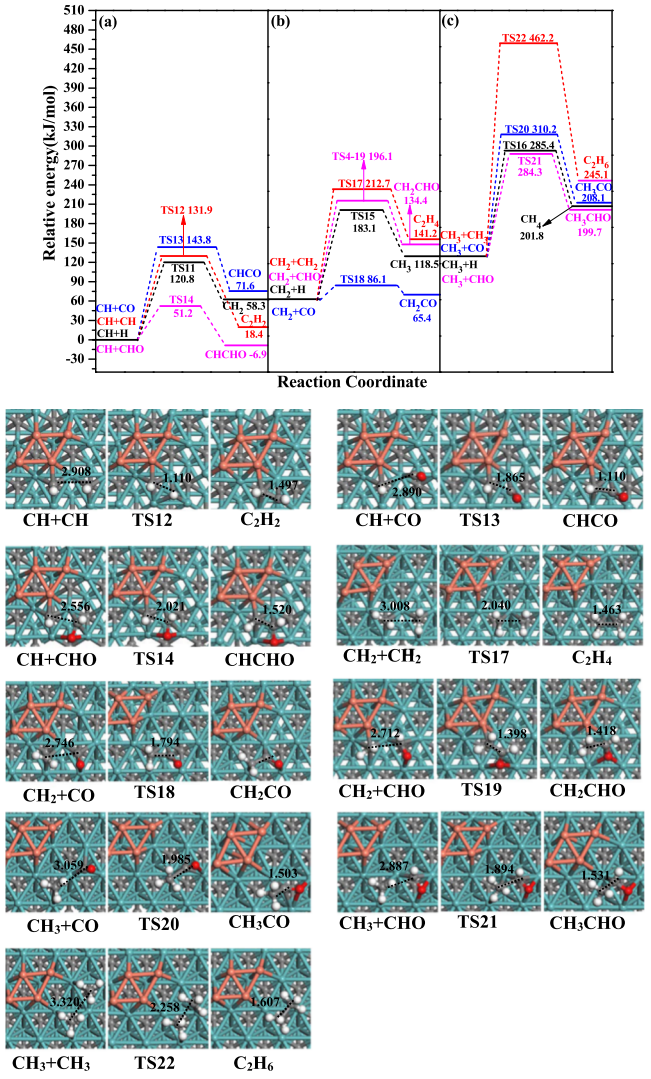

Figure 5. Potential energy diagram for the related reactions of (a) CH, (b) CH_2, and (c) CH_3 species together with the structures of the initial state, transition state, and final state on the Cu/β-Mo_2C(001) surface. Bond lengths are in Å. See Figure 2 for color coding.

reaction of the CH species prefers to occur at the interface because of the preferential adsorption of the CH species at the interface. The CHO reaction with CH to form CHCHO is the most preferred with the activation free energy of 51.2 kJ·mol^{-1}. The activation free energies of CO reaction with CH, CH self-coupling to C_2H_2, and CH hydrogenation to CH_2 are 143.8, 131.9, and 120.8 kJ·mol^{-1}, respectively. Therefore, C_2 oxygenate CHCHO is the main product among the related reactions of CH. However, as the reactions of CO hydrogenations to CHO and CO direct dissociation are two parallel routes, one part of CO is responsible for the formation of CH by CO direct dissociation and hydrogenation, and the other part of CO is responsible for CHO formation by CO hydrogenation.

In addition, as shown in Figure 5b, the related reactions of CH_2 species show that CH_2 reaction with CO to CH_2CO is the easiest with the activation free energy of 27.8 kJ·mol^{-1}; namely, C_2 oxygenates are the main product when CH_2 is the preferred CH_x species. Meanwhile, CH_3 dissociation into CH_2 is the most favorable among all related reactions of the CH_3 species (Figure 5c); namely, once CH_3 is formed, it prefers to be dissociated into CH_2 with an activation free energy of 64.6 kJ·mol^{-1}. Namely, only CH and CH_2 species exist over Cu/β-Mo_2C(001).

On the basis of the above analysis, over the Cu/β-Mo_2C(001) surface, once the CH_3 species is formed, it prefers to be dissociated into CH_2; namely, only CH and CH_2 species exist over Cu/β-Mo_2C(001). Moreover, the CH monomer acted as the most preferred CH_x species dominantly participating in the formation of C_2 oxygenate CHCHO instead of its coupling to C_2 hydrocarbons; meanwhile, a small quantity of CH species may be hydrogenated to form CH_2, which also contributes to the formation of C_2 oxygenate CH_2CO by CO reaction with CH_2 instead of its coupling to C_2 hydrocarbons. Thus, C_2 oxygenates are the dominant product instead of the hydrocarbons (C_2H_2, C_2H_4, C_2H_6, and CH_4) over Cu/β-Mo_2C(001).

In addition, the work by Rodriguez et al.[34] experimentally and theoretically investigated the selectivity and activity of an admetal induced over the orthorhombic β-Mo_2C and Cu/β-Mo_2C catalysts for the conversion of CO_2 to methanol, suggesting that the interaction of CO_2 with the supported Cu clusters catalysts was weaker than that with the pure β-Mo_2C catalyst, and subsequently the dissociation energy barrier is much higher than the desorption energy, in agreement with the experimental results that the amount of detected CO decreases when the Cu coverage increases. However, in our study, CO prefers to be adsorbed via the C atom at the interface site between Cu and β-Mo_2C over Cu/β-Mo_2C catalysts; the energy barriers of CO desorption are higher than CO dissociation or CO hydrogenation to CHO (193.9 vs 116.4 and 116.8 kJ·mol^{-1}). On the contrary, Rodriguez et al. only investigated the interaction of CO with the supported Cu clusters, which was weaker than that at the interface site between Cu and β-Mo_2C in our study, and therefore the dissociation energy barrier of CO is much higher than the desorption energy, which is not in favor of C_2 oxygenates. Thus, the whole reaction of CO_2 hydrogenation to methanol over the Cu/β-Mo_2C(001) surface occurred at a rather high CO partial pressure may be needed in the studies by Rodriguez et al. Further, it is believed that the moderate catalytic activity of CH formation at the interface site between Cu and β-Mo_2C on the Cu/β-Mo_2C(001) surface realizes a balance between CHO/CO dissociation into CH species and the undissociated CO/CHO species, and facilitates C_2 oxygenate formation via the undissociated CHO insertion into CH, thereby promoting C_2 oxygenate formation with high selectivity.

3.5. CH_4 Formation and Its Effect on C_2 Oxygenate Formation. As shown in Figure 5, starting with CH, the overall barrier of CH_4 formation is 285.4 kJ·mol^{-1} on Cu/β-Mo_2C(001). CHCHO and CH_2CO are the preferred C_2 oxygenates with the overall barriers of 51.2 and 86.1 kJ·mol^{-1}, respectively. Hence, Cu/β-Mo_2C(001) presents higher selectivity toward C_2 oxygenates than CH_4. Theoretical and experimental results[20,21] have also confirmed that the hydro-

DOI: 10.1021/acs.jpcc.9b05963
J. Phys. Chem. C 2019, 123, 21022−21030

carbons were the main products in syngas conversion on the Mo_2C catalyst; namely, compared to the Mo_2C catalyst, the role of Cu in Cu/β-Mo_2C(001) inhibits the formation of the hydrocarbons, and promotes the formation of C_2 oxygenates, which agree with the characteristics of the Cu catalyst that the formation of C_2 oxygenates was easy once the CH_x species was formed.[3]

3.6. Analysis of Electronic and Structural Properties. In order to understand the properties of Cu/β-Mo_2C(001) catalysts at an electronic level, we analyzed the plotted charge density difference of the Cu/β-Mo_2C(001) surface, as presented in Figure 6; the results show that the electron

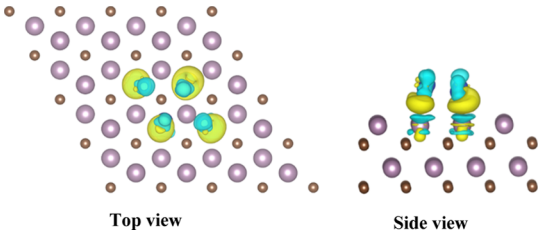

Figure 6. Differential charge density of the Cu/β-Mo_2C(001) surface. The blue and yellow shaded regions represent the charge loss and charge gain, respectively.

transfer occurs between Cu and Mo_2C, and the charge gathers at the interface. Bader charge analysis shows that the total charge transfer from Mo_2C to Cu is 0.6*e*. Hence, the analysis of electronic and structural properties indicates that there is a strong charge transfer between Cu and Mo_2C to form a charge-rich region at the interface of the Cu/β-Mo_2C(001) catalyst, which improves the catalytic performance toward syngas conversion to C_2 oxygenates.

On the other hand, the structural properties of the adsorption site of related species and the sites where the reaction occurs are systematically analyzed; the results show that CO preferentially adsorbs at the interface of the Cu/β-Mo_2C(001) catalyst and promotes its dissociation. The process of CH and CH_2 formation as well as CHO insertion into CH to CHCHO also occur at the interface of the Cu/β-Mo_2C(001) catalyst, and the most stable adsorption sites of C, CH, and CH_2 species are all at the interface of Cu/β-Mo_2C(001). Meanwhile, CO and CHO dissociation also occurs at the interface of Cu/β-Mo_2C(001), which reveals that the interface promotes C−O bond cleavage of CO and CHO to form the CH monomer. However, CHO hydrogenation to form CH_2O, CH_3O, and CH_3OH that occurred at the Mo_2C surface of Cu/β-Mo_2C(001) does not favor the formation of methanol, which is in agreement with the characteristics of the β-Mo_2C catalyst that is in favor of the C−O bond cleavage to form CH_x species, followed by its coupling to form hydrocarbons.[18−22]

In conclusion, the interface of the Cu/β-Mo_2C(001) catalyst could promote the formation of the dominant monomer CH and the subsequent CHO insertion into CH to form C_2 oxygenates, in which β-Mo_2C(001) can suppress methanol formation; Cu is in favor of the presence of undissociated CO/CHO species. As a result, the synergistic effect including electronic effect and geometric effect between Cu and β-Mo_2C(001) leads to high productivity toward C_2 oxygenates in syngas conversion over the Cu/β-Mo_2C(001) catalyst. Our results can provide a valuable clue for the design and optimization of Cu/Mo_2C catalysts in syngas conversion to form C_2 oxygenates with better catalytic performance.

4. CONCLUSIONS

In this study, the mechanism of syngas conversion to C_2 oxygenates over the Cu/β-Mo_2C(001) catalyst has been systematically investigated using the DFT method. The results show that CO initial activation dominantly occurs by CO hydrogenation to CHO and CO direct dissociation. Compared to the pure β-Mo_2C(001), Cu/β-Mo_2C(001) enhances the catalytic activity of CO initial activation. The CH monomer is the most preferred CH_x species on the Cu/Mo_2C catalyst, which is dominantly formed by CO direct dissociation into C, followed by its hydrogenation to CH. Moreover, CH formation is more preferred over methanol formation both thermodynamically and dynamically. Starting from the CH monomer, CHCHO formed by CHO reaction with CH is the dominant C_2 oxygenate, which is favorable in kinetics than other related reactions of the CH species. The analysis of electronic and structural properties indicates that there is a strong charge transfer between Cu and Mo_2C to form a charge-rich region at the interface of the Cu/β-Mo_2C(001) catalyst; meanwhile, the structural properties show that CO, C, CH, and CH_2 species are all preferentially adsorbed at the interface of the Cu/β-Mo_2C(001) catalyst; CH formation and CHO reaction with CH to CHCHO also occur at the interface of the Cu/β-Mo_2C(001) catalyst; namely, the interface promotes C−O bond cleavage of CO and CHO to form the CH monomer, as well as CHO reaction with CH to form CHCHO. However, CHO hydrogenation to form CH_2O, CH_3O, and CH_3OH that occurred at the Mo_2C surface of Cu/β-Mo_2C(001) does not favor the formation of methanol. Therefore, the interface of the Cu/β-Mo_2C(001) catalyst could promote the formation of the dominant monomer CH and the subsequent CHO insertion into CH to form C_2 oxygenates, in which β-Mo_2C(001) suppresses methanol formation; Cu is in favor of the presence of undissociated CO/CHO species.

■ ASSOCIATED CONTENT

Supporting Information

The Supporting Information is available free of charge on the ACS Publications website at DOI: 10.1021/acs.jpcc.9b05963.

Detailed descriptions about the key parameters and the stable configurations of all possible adsorbed species on the Cu/β-Mo_2C(001) surface, the calculation method of Gibbs free energy, and the partial reactions on the β-Mo_2C(001) surface (PDF)

■ AUTHOR INFORMATION

Corresponding Author

*E-mail: wangbaojun@tyut.edu.cn, wbj@tyut.edu.cn.

ORCID

Baojun Wang: 0000-0002-9069-6720

Debao Li: 0000-0002-6891-4787

Notes

The authors declare no competing financial interest.

■ ACKNOWLEDGMENTS

This work is financially supported by the Key projects of National Natural Science Foundation of China (no. 21736007), the National Natural Science Foundation of

DOI: 10.1021/acs.jpcc.9b05963
J. Phys. Chem. C 2019, 123, 21022−21030

China (no. 21776193, 21476155), and the Top Young Innovative Talents of Shanxi.

REFERENCES

(1) Subramani, V.; Gangwal, S. K. A Review of Recent Literature to Search for an Efficient Catalytic Process for the Conversion of Syngas to Ethanol. *Energ. Fuel.* **2008**, *22*, 814−839.

(2) Fang, K.; Li, D.; Lin, M.; Xiang, M.; Wei, W.; Sun, Y. A Short Review of Heterogeneous Catalytic Process for Mixed Alcohols Synthesis via Syngas. *Catal. Today* **2009**, *147*, 133−138.

(3) Gupta, M.; Smith, M. L.; Spivey, J. J. Heterogeneous Catalytic Conversion of Dry Syngas to Ethanol and Higher Alcohols on Cu-Based Catalysts. *ACS Catal* **2011**, *1*, 641−656.

(4) Yue, H. R.; Ma, X. B.; Gong, J. L. An Alternative Synthetic Approach for Efficient Catalytic Conversion of Syngas to Ethanol. *Acc. Chem. Res.* **2014**, *47*, 1483−1492.

(5) Gong, J. L.; Yue, H. R.; Zhao, Y. J.; Zhao, S.; Zhao, L.; Lv, J.; Wang, S. P.; Ma, X. B. Synthesis of Ethanol via Syngas on Cu/SiO_2 Catalysts with Balanced Cu^0-Cu^+ Sites. *J. Am. Chem. Soc.* **2012**, *134*, 13922−13925.

(6) Choi, Y. M.; Liu, P. Mechanism of Ethanol Synthesis from Syngas on Rh(111). *J. Am. Chem. Soc.* **2009**, *131*, 13054−13061.

(7) Mei, D. H.; Rousseau, R.; Kathmann, S. M.; Glezakou, V. A.; Engelhard, M. H.; Jiang, W. L.; Wang, C. M.; Gerber, M. A.; White, J. F.; Stevens, D. J. Ethanol Synthesis from Syngas over Rh-Based/SiO_2 Catalysts: A Combined Experimental and Theoretical Modeling Study. *J. Catal.* **2010**, *271*, 325−342.

(8) Surisetty, V. R.; Dalai, I. E. A. K. Comparative Study of Higher Alcohols Synthesis over Alumina and Activated Carbon-Supported Alkali-Modified MoS_2 Catalysts Promoted with Group VIII Metals. *Fuel* **2012**, *96*, 77−84.

(9) Prieto, G.; Beijer, S.; Smith, M. L.; He, M.; Au, Y.; Wang, Z.; Bruce, D. A.; de Jong, K. P.; Spivey, J. J.; de Jongh, P. E. Design and Synthesis of Copper−Cobalt Catalysts for the Selective Conversion of Synthesis Gas to Ethanol and Higher Alcohols. *Angew. Chem., Int. Ed.* **2014**, *53*, 6397−6401.

(10) Subramanian, N. D.; Balaji, G.; Kumar, C. S. S. R.; Spivey, J. J. Development of Cobalt−Copper Nanoparticles as Catalysts for Higher Alcohol Synthesis from Syngas. *Catal. Today* **2009**, *147*, 100−106.

(11) Bao, Z. H.; Xiao, K.; Qi, X. Z.; Wang, X. X.; Zhong, L. S.; Fang, K. G.; Lin, M. G.; Sun, Y. H. Higher Alcohol Synthesis over Cu-Fe Composite Oxides with High Selectivity to $C_{2+}OH$. *J. Energy Chem.* **2013**, *22*, 107−113.

(12) Sun, H. Study on the Reaction Mechanism of Ethanol Synthesis from on Cu Catalyst. Ms.D. Thesis, TaiyuanUniversity of Technology, 2013, June.

(13) Sun, X. C.; Zhang, R. G.; Wang, B. J. Insights into the Preference of CH_x(x=1−3) Formation from CO Hydrogenation on Cu(111) Surface. *Appl. Surf. Sci.* **2013**, *265*, 720−730.

(14) Zhang, R.; Sun, X.; Wang, B. Insight into the Preference Mechanism of CH_x(x=1-3) and C-C Chain Formation Involved in C_2 Oxygenate Formation from Syngas on the Cu(110) Surface. *J. Phys. Chem. C* **2013**, *117*, 6594−6606.

(15) Zheng, H. Y.; Zhang, R. G.; Li, Z.; Wang, B. J. Insight into the Mechanism and Possibility of Ethanol Formation from Syngas on Cu(100) Surface. *J. Mol. Catal. A: Chem.* **2015**, *404*, 115−130.

(16) Sun, J.; Cai, Q. X.; Wan, Y.; Wan, S. L.; Wang, L.; Lin, J. D.; Mei, D. H.; Wang, Y. Promotional Effects of Cesium Promoter on Higher Alcohol Synthesis from Syngas over Cesium-Promoted Cu/ZnO/Al_2O_3 Catalysts. *ACS Catal.* **2016**, *6*, 5771−5785.

(17) Zhao, Y.-H.; Yang, M. M.; Sun, D. P.; Su, H. Y.; Sun, K. J.; Ma, X. F.; Bao, X. H.; Li, W. X. Rh-Decorated Cu Alloy Catalyst for Improved C_2 Oxygenate Formation from Syngas. *J. Phys. Chem. C* **2011**, *115*, 18247−18256.

(18) Ao, M.; Pham, G. H.; Sunarso, J.; Tade, M. O.; Liu, S. M. Active Centers of Catalysts for Higher Alcohol Synthesis from Syngas: A Review. *ACS Catal.* **2018**, *8*, 7025−7050.

(19) Wu, W. C.; Wu, Z. L.; Liang, C. H.; Chen, X. W.; Ying, P. L.; Li, C. In Situ FT-IR Spectroscopic Studies of CO Adsorption on Fresh Mo_2C/Al_2O_3 Catalyst. *J. Phys. Chem. B* **2003**, *107*, 7088−7094.

(20) Shou, H.; Ferrari, D.; Barton, D. G.; Jones, C. W.; Davis, R. J. Influence of Passivation on the Reactivity of Unpromoted and Rb Promoted Mo_2C Nanoparticles for CO Hydrogenation. *ACS Catal.* **2012**, *2*, 1408−1416.

(21) Li, L.; Sholl, D. S. Computational Identification of Descriptors for Selectivity in Syngas Reactions on a Mo_2C Catalyst. *ACS Catal.* **2015**, *5*, 5174−5185.

(22) Ranhotra, G. S.; Bell, A. T.; Reimer, J. A. Catalysis over Molybdenum Carbides and Nitrides: II. Studies of CO Hydrogenation and C_2H_6 Hydrogenolysis. *J. Catal.* **1987**, *108*, 40−49.

(23) Christensen, J. M.; Duchstein, L. D. L.; Wagner, J. B.; Jensen, P. A.; Temel, B.; Jensen, A. D. Catalytic Conversion of Syngas into Higher Alcohols over Carbide Catalysts. *Ind. Eng. Chem. Res.* **2012**, *51*, 4161−4172.

(24) Hu, J. L.; Wang, Y.; Cao, C. S.; Elliott, D. C.; Stevens, D. J.; White, J. F. Conversion of Biomass-Derived Syngas to Alcohols and C_2 Oxygenates Using Supported Rh Catalysts in a Microchannel Reactor. *Catal. Today* **2007**, *120*, 90−95.

(25) Farmer, J. A.; Campbell, C. T. Ceria Maintains Smaller Metal Catalyst Particles by Strong Metal-Support Bonding. *Science* **2010**, *329*, 933−936.

(26) Pan, Y. X.; Liu, M.; Ge, Q. F. Effect of Surface Hydroxyls on Selective CO_2 Hydrogenation over Ni_4/γ-Al_2O_3: A Density Functional Theory Study. *J. Catal.* **2010**, *272*, 227−234.

(27) Ngo, H.; Liu, Y. Y.; Murata, K. Effect of Secondary Additives (Li, Mn) in Fe-Promoted Rh/TiO_2 Catalysts for the Synthesis of Ethanol from Syngas. *React. Kinet., Mech. Catal.* **2011**, *102*, 425−435.

(28) Rodríguez, J. A.; Evans, J.; Graciani, J.; Park, J. B.; Liu, P.; Hrbek, J.; Sanz, J. F. High Water-Gas Shift Activity in TiO_2(110) Supported Cu and Au Nanoparticles: Role of the Oxide and Metal Particle Size. *J. Phys. Chem. C* **2009**, *113*, 7364−7370.

(29) Bai, H.; Ma, M. M.; Ramírez, B.; Cao, H. J.; Zhang, L.; Park, Z. H.; Vinokurov, V. A.; Huang, W. Carbon Chain Growth by Formyl Coupling over the Cu/γ-AlOOH(001) Surface in Syngas Conversion. *Phys. Chem. Chem. Phys.* **2019**, *21*, 148−159.

(30) Bai, B.; Bai, H.; Zhang, L.; Huang, W. Catalytic Activity of γ-AlOOH(001) Surface in Syngas Conversion: Probing into the Mechanism of Carbon Chain Growth. *Appl. Surf. Sci.* **2018**, *455*, 123−131.

(31) Yang, Y. X.; Evans, J.; Rodriguez, J. A.; White, M. G.; Liu, P. Fundamental Studies of Methanol Synthesis from CO_2 Hydrogenation on Cu(111), Cu Clusters, and Cu/ZnO(000-1). *Phys. Chem. Chem. Phys.* **2010**, *12*, 9909−9917.

(32) Bruix, A.; Rodriguez, J. A.; Ramírez, P. J.; Senanayake, S. D.; Evans, J.; Park, J. B.; Stacchiola, D.; Liu, P.; Hrbek, J.; Illas, F. A New Type of Strong Metal−Support Interaction and the Production of H_2 through the Transformation of Water on Pt/CeO_2(111) and Pt/CeO_x/TiO_2(110) Catalysts. *J. Am. Chem. Soc.* **2012**, *134*, 8968−8974.

(33) Zhang, R. G.; Wen, G. X.; Adidharma, H.; Russell, A. G.; Wang, B. J.; Radosz, M.; Fan, M. H. C_2 Oxygenate Synthesis via Fischer−Tropsch Synthesis on Co_2C and Co/Co_2C Interface Catalysts: How To Control the Catalyst Crystal Facet for Optimal Selectivity. *ACS Catal.* **2017**, *7*, 8285−8295.

(34) Posada-Pérez, S.; Ramírez, P. J.; Gutiérrez, R. A.; Stacchiola, D. J.; Viñes, F.; Liu, P.; Illasa, F.; Rodriguez, J. A. The Conversion of CO_2 to Methanol on Orthorhombic β-Mo_2C and Cu/β-Mo_2C Catalysts: Mechanism for Admetal Induced Change in the Selectivity and Activity. *Catal. Sci. Technol.* **2016**, *6*, 6766−6777.

(35) Lu, Y. W.; Zhang, R. G.; Cao, B. B.; Ge, B. H.; Tao, F. F.; Shan, J. J.; Nguyen, L.; Bao, Z. H.; Wu, T. P.; Pote, J. W.; et al. Elucidating the Copper-Hägg Iron Carbide Synergistic Interactions for Selective CO Hydrogenation to Higher Alcohols. *ACS Catal.* **2017**, *7*, 5500−5512.

(36) Zhou, J.; Mullins, D. R. Rh-Promoted Methanol Decomposition on Cerium Oxide Thin Films. *J. Phys. Chem. B* **2006**, *110*, 15994−16002.

DOI: 10.1021/acs.jpcc.9b05963
J. Phys. Chem. C 2019, 123, 21022−21030

(37) Chen, T.-Y.; Su, J. J.; Zhang, Z. P.; Cao, B.; Wang, X.; Si, R.; Liu, X. L.; Shi, B. F.; Xu, J.; Han, Y. F. Structure Evolution of Co−CoO_x Interface for Higher Alcohol Synthesis from Syngas over Co/CeO_2 Catalysts. *ACS Catal.* **2018**, *8*, 8606−8617.
(38) Pei, Y. P.; Liu, J. X.; Zhao, Y. H.; Ding, X.; Liu, T.; Dong, W. D.; Zhu, H. J.; Su, H. Y.; Yan, L.; Li, J. L.; et al. High Alcohols Synthesis via Fischer−Tropsch Reaction at Cobalt Metal/Carbide Interface. *ACS Catal.* **2015**, *5*, 3620−3624.
(39) Xiang, M. L.; Li, D. B.; Xiao, H. C.; Zhang, J. L.; Qi, H. J.; Li, W. H.; Zhong, B.; Sun, Y. H. Synthesis of Higher Alcohols from Syngas over Fischer-Tropsch Elements Modified K/β-Mo_2C Catalysts. *Fuel* **2008**, *87*, 599−603.
(40) Dong, J.; Fu, Q.; Jiang, Z.; Mei, B. B.; Bao, X. H. Carbide-Supported Au Catalysts for Water−Gas Shift Reactions: A New Territory for the Strong Metal−Support Interaction Effect. *J. Am. Chem. Soc.* **2018**, *140*, 13808−13816.
(41) Schweitzer, N. M.; Schaidle, J. A.; Ezekoye, O. K.; Pan, X. Q.; Linic, S.; Thompson, L. T. High Activity Carbide Supported Catalysts for Water Gas Shift. *J. Am. Chem. Soc.* **2011**, *133*, 2378−2381.
(42) Posada-Pérez, S.; Viñes, F.; Rodríguez, J. A.; Illas, F. Structure and Electronic Properties of Cu Nanoclusters Supported on Mo_2C(001) and Mo_2C(001) Surfaces. *J. Chem. Phys.* **2015**, *143*, 114704.
(43) Zhao, Y.-H.; Chen, J. G.; Ma, X. F.; Liu, J. X.; Sun, D. P.; Su, H. Y.; Li, W. X. Carbon Chain Growth by Formyl Insertion on Rhodium and Cobalt Catalysts in Syngas Conversion. *Angew. Chem., Int. Ed.* **2011**, *50*, 5335−5338.
(44) Schweicher, J.; Viñes, A.; Kruse, N. Hydrocarbon Chain Lengthening in Catalytic CO Hydrogenation: Evidence for a CO-Insertion Mechanism. *J. Am. Chem. Soc.* **2012**, *134*, 16135−16138.
(45) Solymosi, F.; Oszkó, L.; Bánsági, T.; Tolmacsov, P. Adsorption and Reaction of CO_2 on Mo_2C Catalyst. *J. Phys. Chem. B* **2002**, *106*, 9613−9618.
(46) Kelly, T. G.; Chen, J. G. G. Controlling C−O, C−C. and C−H. Bond Scission for Deoxygenation, Reforming, and Dehydrogenation of Ethanol using Metal-Modified Molybdenum Carbide Surfaces. *Green Chem.* **2014**, *16*, 777−784.
(47) Politi, J. R. d. S.; Viñes, F.; Rodriguez, J. A.; Illas, F. Atomic and Electronic Structure of Molybdenum Carbide Phases: Bulk and Low Miller-index Surfaces. *Phys. Chem. Chem. Phys.* **2013**, *15*, 12617−12625.
(48) Han, J. W.; Li, L. W.; Sholl, D. S. Density Functional Theory Study of H and CO Adsorption on Alkali-Promoted Mo_2C Surfaces. *J. Phys. Chem. C* **2011**, *115*, 6870−42.
(49) Ren, J.; Huo, C. F.; Wang, J. G.; Li, Y. W.; Jiao, H. J. Surface Structure and Energetics of Oxygen and CO Adsorption on α-Mo_2C(0001). *Surf. Sci.* **2005**, *596*, 212−221.
(50) Tominaga, H.; Nagai, M. Density Functional Theory of Water-Gas Shift Reaction on Molybdenum Carbide. *J. Phys. Chem. B* **2005**, *109*, 20415−20423.
(51) Tominaga, H.; Nagai, M. Theoretical Study of Methane Reforming on Molybdenum Carbide. *Appl. Catal., A* **2007**, *328*, 35−41.
(52) Tominaga, H.; Nagai, M. Mechanism of Thiophene Hydrodesulfurization on Clean/Sulfided β-Mo_2C(001) based on Density Functional Theory—*cis*- and *trans*-2-Butene Formation at the Initial Stage. *Appl. Catal., A* **2008**, *343*, 95−103.
(53) Posada-Pérez, S.; Viñes, F.; Ramirez, P. J.; Vidal, A. B.; Rodriguez, J. A.; Illas, F. The Bending Machine: CO_2 Activation and Hydrogenation on δ-MoC(001) and β-Mo_2C(001) Surfaces. *Phys. Chem. Chem. Phys.* **2014**, *16*, 14912−14921.
(54) Kresse, G.; Hafner, J. Ab Initio Molecular Dynamics for Liquid Metals. *Phys. Rev. B: Condens. Matter Mater. Phys.* **1993**, *47*, 558−561.
(55) Stadler, R.; Wolf, W.; Podloucky, R.; Kresse, G.; Furthmüller, J.; Hafner, J. Ab Initio Calculations of the Cohesive, Elastic, and Dynamical Properties of $CoSi_2$ by Pseudopotential and All-Electron Techniques. *Phys. Rev. B: Condens. Matter Mater. Phys.* **1996**, *54*, 1729−1734.
(56) Perdew, J. P.; Jónsson, K.; Ernzerhof, M. Generalized Gradient Approximation Made Simple. *Phys. Rev. Lett.* **1996**, *77*, 3865−3868.
(57) Kresse, G.; Furthmüller, J. Efficiency of Ab-Initio Total Energy Calculations for Metals and Semiconductors Using a Plane-Wave Basis set. *Comput. Mater. Sci.* **1996**, *6*, 15−50.
(58) Monkhorst, H. J.; Jónsson, J. D. Special Points for Brillonin-Zone Integrations. *Phys. Rev. B: Condens. Matter Mater. Phys.* **1976**, *13*, 5188−5192.
(59) Henkelman, G.; Jónsson, H. A Dimer Method for Finding Saddle Points on High Dimensional Potential Surfaces Using only First Derivatives. *J. Chem. Phys.* **1999**, *111*, 7010−7022.
(60) Olsen, R. A.; Kroes, G. J.; Henkelman, G.; Arnaldsson, A.; Jónsson, H. Comparison of Methods for Finding Saddle Points without Knowledge of the Final States. *J. Chem. Phys.* **2004**, *121*, 9776−9792.
(61) Henkelman, G.; Jónsson, H. Improved Tangent Estimate in the Nudged Elastic Band Method for Finding Minimum Energy Paths and Saddle Points. *J. Chem. Phys.* **2000**, *113*, 9978−9985.
(62) Henkelman, G.; Uberuaga, B. P.; Jónsson, H. A Climbing Image Nudged Elastic Band Method for Finding Saddle Points and Minimum Energy Paths. *J. Chem. Phys.* **2000**, *113*, 9901−9904.
(63) Xu, X.-C.; Su, J. J.; Tian, G.-C.; Fu, D. L.; Dai, W. W.; Mao, W.; Yuan, W. K.; Xu, J.; Han, Y. F. First-Principles Study of C_2 Oxygenates Synthesis Directly From Syngas over CoCu Bimetallic Catalysts. *J. Phys. Chem. C* **2015**, *119*, 216−227.
(64) Ren, B. H.; Dong, X. Q.; Yu, Y. Z.; Wen, G. B.; Zhang, M. H. A Density Functional Theory Study on the Carbon Chain Growth of Ethanol Formation on Cu-Co (111) and (211) Surfaces. *Appl. Surf. Sci.* **2017**, *412*, 374−384.
(65) Zhang, R. G.; Wang, G. R.; Wang, B. J.; Ling, L. X. Insight into the Effect of Promoter Mn on Ethanol Formation from Syngas on a Mn-Promoted MnCu(211) Surface: A Comparison with a Cu(211) Surface. *J. Phys. Chem. C* **2014**, *118*, 5243−5254.
(66) Wang, W.; Wang, Y.; Wang, G. C. Ethanol Synthesis from Syngas over Cu(Pd)-doped Fe(100): A Systematic Theoretical Investigation. *Phys. Chem. Chem. Phys.* **2018**, *20*, 2492−2507.

DOI: 10.1021/acs.jpcc.9b05963
J. Phys. Chem. C 2019, 123, 21022−21030